

SUPPLEMENTARY MATERIAL

Solution epitaxy and photoelectric detection performance of halide-oxide perovskite heterojunction

Rong Wu, Jie Tu, Xudong Liu, Xiuqiao Liu, Guoqiang Xi, Jianjun Tian, and Linxing
Zhang*

Institute for Advanced Materials Technology, University of Science and Technology
Beijing, Beijing 100083, China

*Corresponding author: Prof. Linxing Zhang; E-mail address:

linxingzhang@ustb.edu.cn

Tel: 010-65741965

Address: Institute for Advanced Materials Technology, University of Science and
Technology Beijing, 30 Xueyuan Road, Beijing 100083, China

SUPPLEMENTARY MATERIAL

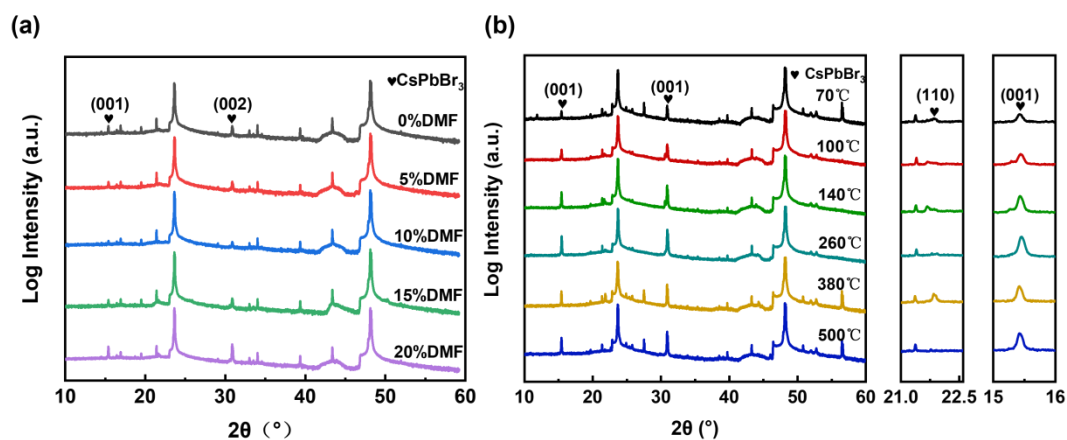


Fig. S1. (a) XRD spectrum of DMF at different addition ratios. At 70 °C annealing, the main diffraction peaks of the film are gradually enhanced with increasing proportion. (b) XRD spectrum at different annealing temperatures.

The determination of the optimal amount of DMF solvent and the annealing temperature of the subsequent process is depicted in the **Fig. S1**. As the amount of DMF is added, the crystallinity gradually increases, but when the content of DMF exceeds 20%, it will cause the precursor solution to be insoluble. When the annealing temperature gradually increases from 70 °C, the crystallinity of the film increases, and when annealed at 260 °C, the (110) plane disappears, and the film only grows preferentially in the (001) orientation. When the annealing temperature continues to increase, although the crystallinity does not weaken, the grain gradually increases and the film cannot be continuous, as shown in the figure below. Based on the above situation, the final amount of DMF is determined to be 20%, and the optimal annealing temperature is determined to be 260 °C.

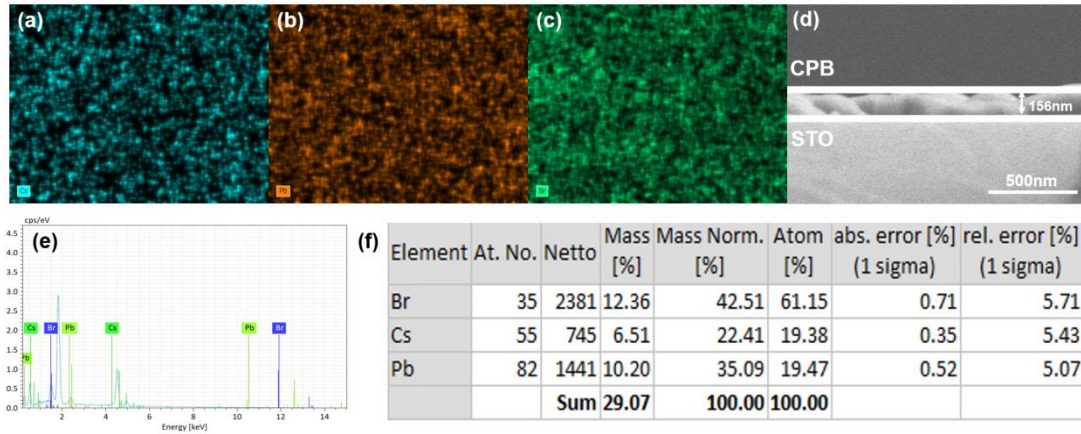


Fig. S2. (a-c) Energy dispersive X-ray spectroscopy (EDS) elemental mapping of the thin film. (d) SEM image of cross-sections of the film. (e, f) EDS shows the atomic ratio of Cs, Pb, and Br in the film is 19.38%: 19.47%: 61.15%.

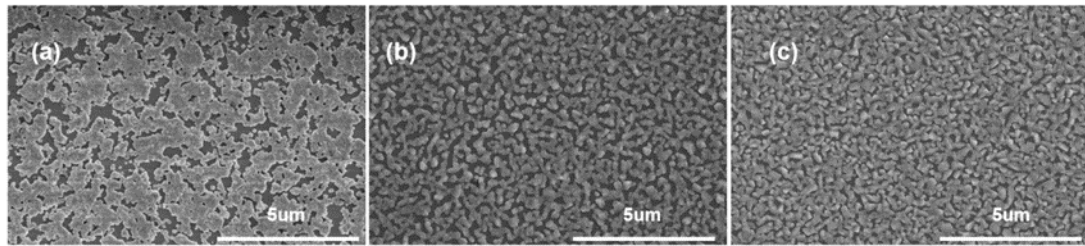


Fig. S3. Extensive SEM images of three films. (a) C1 sample. (b) C2 sample. (c) C3 sample.

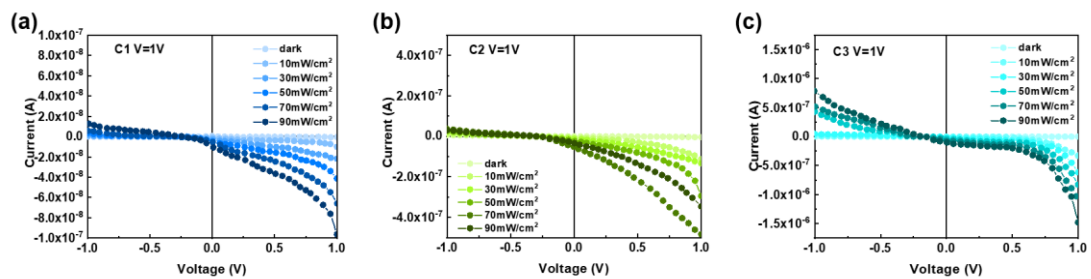


Fig. S4. I - V curves of three CPB-STO devices under white light irradiation at different optical power densities at 1 V bias. (a) C1 sample. (b) C2 sample. (c) C3 sample.

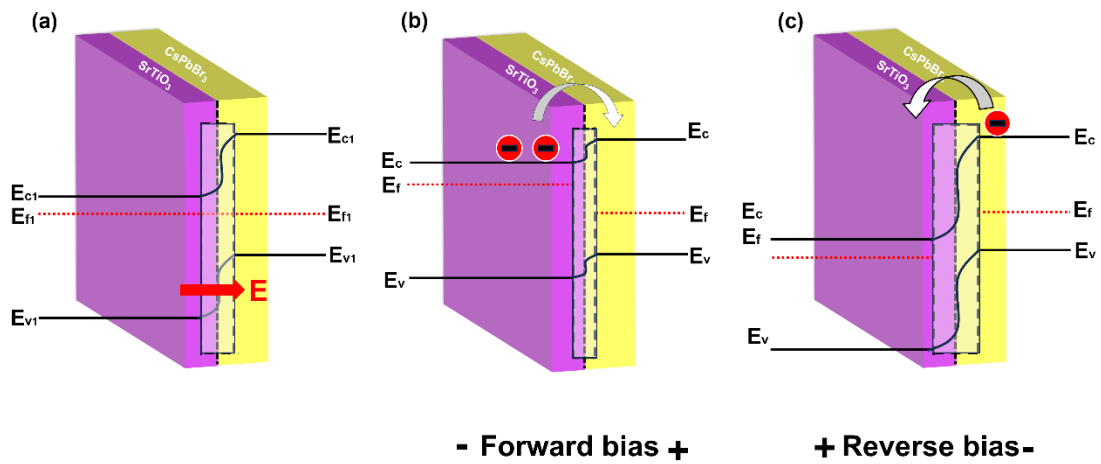


Fig. S5. Structure diagram of CPB - Nb: STO heterojunction energy bands under different biases. (a) No bias. (b) Forward bias. (c) Reverse bias.

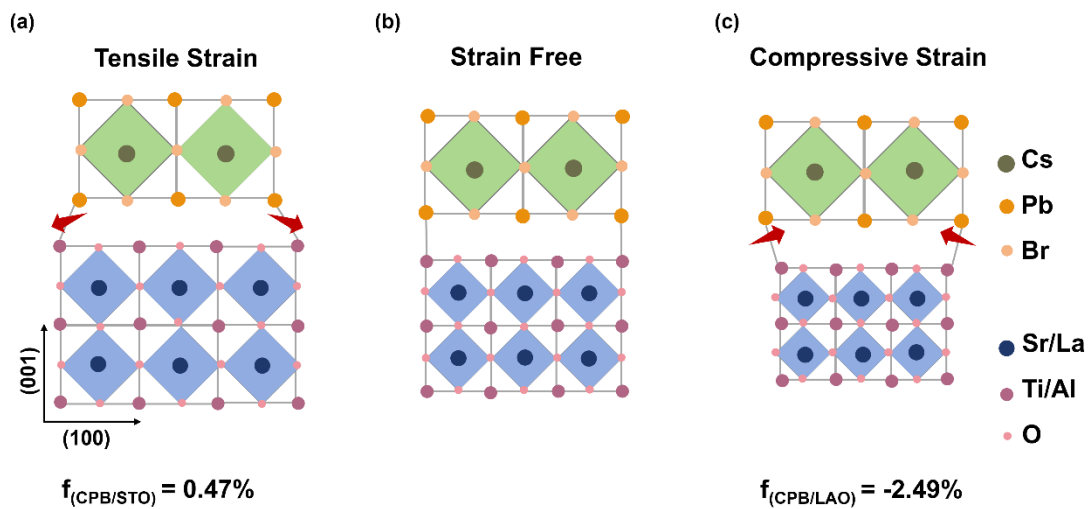


Fig. S6. Schematic representation of the lattice matching relationship of CPB films on STO and LAO substrates. (a) The thin film lattice is smaller than the substrate lattice and exhibits tensile strain. (b) The lattice matches perfectly. (c) The thin film lattice is larger than the substrate lattice and exhibits compressive strain.

Table. S1. The PL lifetime values on C1, C2, C3 thin films and formula for calculating average life.

Table S1. The PL lifetime values on CsPbBr₃ single-film.

	Lifetime τ_1 (ns)	Ratio(%)	Lifetime τ_2 (ns)	Ratio(%)	Average τ (ns)
C1	0.14602	86.31%	1.00722	13.69%	0.264
C2	0.92923	16.48%	2.01233	83.52%	1.834
C3	4.76005	45.12%	5.81784	54.88%	5.342

$$\tau_{avg} = \frac{A_1\tau_1^2 + A_2\tau_2^2 + A_3\tau_3^2}{A_1\tau_1 + A_2\tau_2 + A_3\tau_3}$$

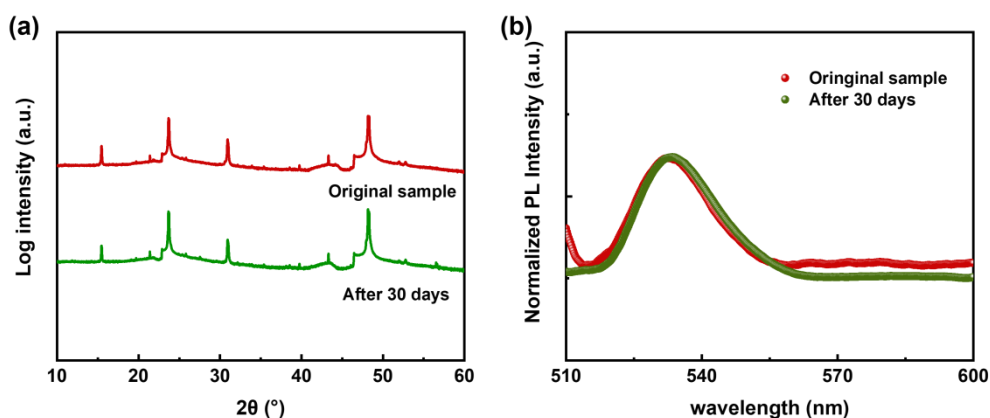


Fig. S7. The long-term stability of the CsPbBr₃ films. (a) XRD spectra and **(b)** PL spectra of the CsPbBr₃ films which have been stored in the ambient environment for one month.

In this paper, we store the prepare CPB films and their devices under ambient conditions. As shown in **Fig. S7(a)**, the XRD intensity and peak position are almost unchanged, and no additional diffraction peaks are shown. There is no obvious loss of photoluminescence (PL) after the film is stored for one month (**Fig. S7(b)**). These results prove the long-term structure and chemical stability of the film. In summary, CPB films show some excellent stability and can be used as promising light trapping materials in practical applications.